2.5D analytical study on ground vibration induced by load moving along a curve

Qincheng Guo and Lintao Xie*

Department of Civil Engineering, Chongqing University, Chongqing, 400000, China

*Corresponding author's e-mail:lintaoxie@cqu.edu.cn

Abstract. In recent years, ground vibration caused by rail transportation has attracted widespread attention, while researches on trains moving along a curve are still limited. To deal with this issue, a curved 2.5D finite element/infinite element approach in the cylindrical coordinate system is proposed to simulate the soil subjected to the moving load on a curved path. Through comparisons with an analytical approach, the proposed model is validated. Some interesting dynamic phenomena of the soil system under the action of curved-path moving load are also found through numerical analyses.

Keywords: 2.5D approach, Finite/infinite element approach, Ground vibration, Centrifugal force, Curved path, Moving load.

1 Introduction

Increasing interest is being shown in the investigation of ground vibration caused by trains for its negative impacts on the surrounding environment of the track, such as residents' normal lives, the accurate use of precision instruments, and so on [1][2]. Significant efforts have been made in the theoretical analysis of ground vibrations over the past few decades. Analytical or semi-analytical methods for the dynamic responses of a homogenous half-space or a multi-layered soil subjected to different moving or non-moving dynamic loads have been presented in previous studies conducted by Lamb [3], Eason [4], de Barros and Luco [5] and Krylov [6] et al., respectively. However, whenever an analytical approach is adopted, assumptions are often made about the geometry and material properties of the ground considered, since closed-form solutions are difficult to obtain for most complex situations.

With the rapid development of computer-aided programming, numerical simulation has been widely applied to research the aforementioned problem. Some scholars, such as De Barros and Luco [5], Taheri [7], He [8] and Wu [9] adopted two-dimensional (2D) and three-dimensional (3D) models to simulate the soil under the action of various forms of loads. However, the 2D model is only suitable for simulating the non-moving loads, while the 3D model is not computationally efficient. To address this issue, Yang and Hung [10] proposed the 2.5-dimensional (2.5D) finite/infinite element approach for simulating train-induced soil vibrations. Assuming that the properties of the half-

P. Xiang et al. (eds.), *Proceedings of the 2023 5th International Conference on Hydraulic, Civil and Construction Engineering (HCCE 2023)*, Atlantis Highlights in Engineering 26,
https://doi.org/10.2991/978-94-6463-398-6_29

space are identical in the load moving direction, the 2D model can effectively simulate the response of the 3D model.

Due to the existing urban layout and various constraints, rail transportation often includes numerous curved sections. Previous studies have mainly focused on investigating the track response [11][12], while relevant researches on the ground vibration [13][14] are limited. Besides, apart from the effect of curvature on response, there is still a lack of research on the impact of centripetal force occurring in the process of trains moving along a curve.

In this paper, a curved 2.5D finite/infinite element approach is proposed to evaluate the vibration of soil induced by the moving load. By deriving the motion equation in the finite element method, the 2.5D finite element/infinite element method in the cylindrical coordinate system is summarized. After the validations of the proposed model, some numerical examples are given to demonstrate the effects of curvature and centrifugal force on the responses.

2 2.5D finite/infinite element approach in cylindrical coordinate system

2.1 Basic assumptions of the problem

As shown in Figure 1, it is assumed that the load moves at velocity c along a curved path with a radius R on the surface of a half-space in a cylindrical coordinate system. It is noted that when the load moves along the curve path, both gravity load T_g (vertically downward) and centrifugal force T_c (horizontally outward) should be considered simultaneously.

$$T_g = mg, \quad T_c = \frac{mc^2}{R} \tag{1}$$

where m is the mass, g is the acceleration of gravity and R is the radius of the curved path.

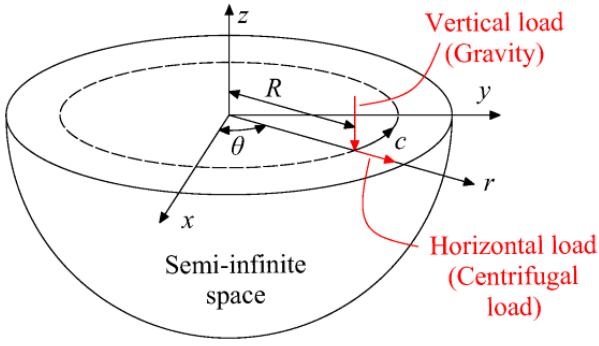

Fig. 1. Load moving along a curve on the surface of a half-space

Since the Fourier transforms and corresponding inverse transforms are required for this approach, their definitions in the present paper are given as

$$\tilde{f}(r,\theta,z,\omega) = \frac{1}{2\pi}\int_{-\infty}^{\infty} f(r,\theta,z,t)\exp(-i\omega t)\,dt$$
$$f(r,\theta,z,t) = \int_{-\infty}^{\infty} \tilde{f}(r,\theta,z,\omega)\exp(i\omega t)\,d\omega \tag{2}$$

Taking vertical loads as an example, the general form of external vertical loads can be expressed as

$$f(r,\theta,z,t) = \psi(r,z)\phi(\theta - \frac{c}{R}t)q(t) \tag{3}$$

where $\psi(r,z)$ represents the distribution function of the moving load on the *r*-*z* plane, $\phi(\theta - ct/R)$ along the θ-axis direction and $q(t)$ denotes the dynamic component of the load which is set herein as:

$$q(t) = T\exp(i\omega_0 t) \tag{4}$$

where ω_0 is the self-oscillation frequency of the moving load.

By performing the Fourier transformation with respect to time *t* to equation (3), the transformed external load is:

$$\tilde{f}(r,\theta,z,\omega) = \frac{R}{c}T\psi(r,z)\tilde{\phi}(-k)\exp(-ik\theta) \tag{5}$$

where $k_\theta = -k = -(\omega - \omega_0)R/c$.

By applying the inverse Fourier transformation to equation (5), the external load in time domain is:

$$f(r,\theta,z,t) = \int_{-\infty}^{\infty}\frac{R}{c}T\psi(r,z)\tilde{\phi}(-k)\exp(-ik\theta)\exp(i\omega t)d\omega \tag{6}$$

The preceding equation shows that the external load can be derived from the integration of a series of harmonic loads.

For a linear system, the total steady-state response of the half-space can be obtained by superposing the responses induced by all harmonic loads. By setting $H(i\omega)$ as the frequency response function for each harmonic load $\psi(r,z)\exp(-ik\theta)\exp(i\omega t)$, the total time-domain response of the half-space is:

$$d(r,\theta,z,t) = \int_{-\infty}^{\infty}\frac{R}{c}T\tilde{\phi}(-k)H(i\omega)\exp(i\omega t)d\omega \tag{7}$$

where $H(i\omega)$ n be obtained by the 2.5D finite/infinite element approach. For the case of the moving point load, $\tilde{\phi}(-k)$ is equal to $1/(2\pi)$.

2.2 Procedure of Derivation for Finite/Infinite Elements

Assume that the material and geometric properties of the half-space system are identical along the θ -axis direction. In response to the external load $\psi(r,z)\exp(-ik\theta)\exp(i\omega t)$, the displacements components, i.e., *u*, *v* and *w* can be expressed as

$$u(r,\theta,z,t) = \hat{u}(r,z)\exp(-ik\theta)\exp(i\omega t)$$
$$v(r,\theta,z,t) = \hat{v}(r,z)\exp(-ik\theta)\exp(i\omega t)$$
$$w(r,\theta,z,t) = \hat{w}(r,z)\exp(-ik\theta)\exp(i\omega t) \tag{8}$$

where $\hat{u},\hat{v},\hat{w}$ denote the displacements of the profile along r,θ,z axes.

According to the principle of virtual displacement, the equations of motion for the half space can be expressed as:

$$\sum[(-\omega^2[M]_e + [K]_e)\{d\}_e - \{p\}_e] = \{0\} \tag{9}$$

where $\{p\}_e$ and $\{d\}_e$ are the node external forces and node displacements vectors of the element, and the stiffness matrix $[K]_e$ and the mass matrix $[M]_e$of the element can be respectively written as:

$$[K]_e = \int\int[\bar{B}]^T[E][B]tJrd\xi d\eta,\ [M]_e = \int\int\rho[N]^T[N]tJrd\xi d\eta \tag{10}$$

where ζ and η denote the two local element coordinates, t denotes the thickness of element, r denotes the global coordinate of the integration point, ρ denotes the density of the material, J denotes the determinant of the Jacobian matrix $[J]$, $[N]$ denotes the shape functions, $[B] = [L][N]$ denotes the strain matrix, $[E]$ denotes the constitutive matrix. Among them, $[E]$ is the same on the cylindrical coordinate axis as that in the Cartesian coordinate system, while $[L]$ can be represented as:

$$[L]^T = \begin{bmatrix} \frac{\partial}{\partial r} & \frac{1}{r} & 0 & 0 & \frac{\partial}{\partial z} & -\frac{ik}{r} \\ 0 & -\frac{ik}{r} & 0 & \frac{\partial}{\partial z} & 0 & \frac{\partial}{\partial r}-\frac{1}{r} \\ 0 & 0 & \frac{\partial}{\partial z} & -\frac{ik}{r} & \frac{\partial}{\partial r} & 0 \end{bmatrix} \tag{11}$$

As shown in Figure 2, the near and far fields of a half space are modeled by the finite (Q8) and infinite (Q5) element, respectively. Since the Q8 finite element is available in most finite element books, only the key features of the Q5 infinite element will be briefed here. For the Q5 infinite element, both the displacement and coordinate shape functions are:

$$N_1 = -\frac{\eta(\eta-1)}{2}e^{-\alpha_i\xi}e^{-ik_i'\xi},\ N_2 = -(\eta-1)(1+\eta)e^{-\alpha_i\xi}e^{-ik_i'\xi}$$
$$N_3 = -\frac{\eta(\eta+1)}{2}e^{-\alpha_i\xi}e^{-ik_i'\xi} \tag{12}$$

$$M_1 = \frac{1}{2}(\xi-1)(\eta-1)\eta,\ M_2 = (\xi-1)(1-\eta)(1+\eta),\ M_3 = -\frac{1}{2}(\xi-1)(1+\eta)\eta$$
$$M_4 = -\frac{1}{2}\xi(\eta-1),\ M_5 = \frac{1}{2}\xi(1+\eta) \tag{13}$$

where α_i is the amplitude decay factor and k_i' the modified wavenumber. The decaying function $e^{-\alpha_i\xi}$ represents the radiation damping caused by waves propagating to infinity, and $e^{-ik_i'\xi}$ the effect of wave oscillation.

For a semi-infinite solid, the waves propagate in the forms of Rayleigh waves, shear waves and compressional waves, as shown in Figure 2, which dominate in different regions. In this case, the amplitude decay factor α_i in equation (12) can be given for each region considered, i.e.,

$$\alpha_R = \frac{1}{2R_\alpha}\frac{k^2}{k^2+k_R^2},\ \alpha_p = \frac{1}{2R_\alpha}+\frac{1}{2R_\alpha}\frac{k^2}{k^2+k_P^2},\ \alpha_s = \frac{1}{2R_\alpha}+\frac{1}{2R_\alpha}\frac{k^2}{k^2+k_S^2} \tag{14}$$

where R_α denotes the distance between the origin (R, 0) and the boundary of the finite element mesh, the $k_i = \omega/c_i$ denotes wavenumber. And the modified wavenumber $k_i{}'$ in equation (14) is represented as $k_i' = [(\omega/c_i)^2 - k_i^2]^{1/2}$.

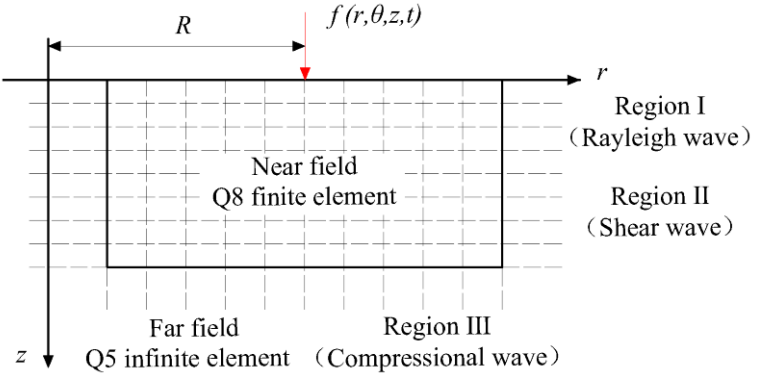

Fig. 2. Finite/infinite element mesh for near and far fields.

The displacements solved from equation (9) should be interpreted as the frequency response function $H(\mathrm{i}\omega)$ for the displacement. Accordingly, the displacement response in time domain can be computed from equation (7) using the inverse Fourier transformation.

3 Model validations

For evaluating the applicability of the present method, the radius of the load's moving trajectory R is set to be large enough, i.e., R = 10000 m, so that the problem considered herein can be approximately regarded as that where the load moves along a straight line. Herein, a uniform viscoelastic half-space subjected to a vertical point load moving along a straight line on the surface with an amplitude $P = 1.6 \times 10^5 N$ and dynamic frequency f_0 = 20 Hz at speed c = 70 m/s is considered. The time t = 0 s corresponds to the moment when the moving load is arriving at $\theta = 0$. The soil characteristics used herein are as follows: Young's modulus E = 50 MPa, Poisson's ratio ν = 0.25, density ρ = 2000 kg/m^3 and damping ratio β = 0.02. Correspondingly, the value of the P, S and Rayleigh wave speeds are 173.2, 100 and 91.8 m/s, respectively. The present method and the analytical one proposed by Yang and Hung [14] are adopted to obtain the vibration responses of the soil for the aforementioned case.

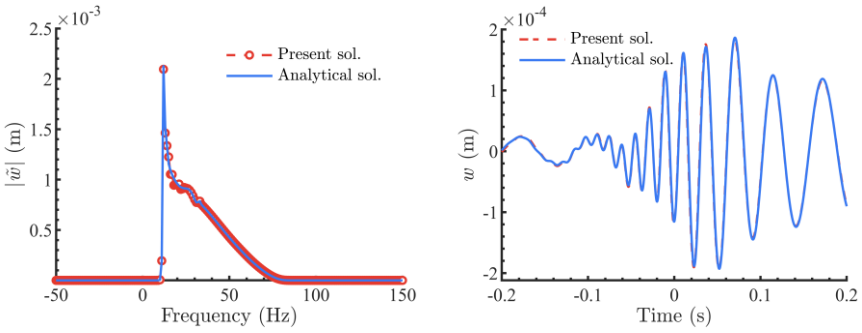

Fig. 3. Comparison of the present results with the analytical ones of Yang and Hung at the observation point O-10 for the case with f_0 = 20 Hz, c = 70 m/s: (a) vertical frequency-domain response; (b) vertical time-domain response

For clarity, the observation points are denoted by the symbols "I-r" and "O-r", where I and O represent the inner and outer sides of the curve movement path, respectively, and r represents the distance from the observation point to the origin (all observation points selected are on the plane of z = 1 m).

The vertical displacements in frequency domain and time domain at the observation point O-10 have been in comparison with the analytical solutions obtained by Yang and Hung's method in Figure 3, in which part (a) shows the magnitude of the vertical displacements with respect to the frequency f and part (b) the real-part vertical displacements in time domain. As can be seen, for this case, the present method agrees exactly with the analytical one in both frequency domain and time domain responses.

4 Calculation examples

Unless otherwise mentioned, the soil characteristics aforementioned are continually used in all the following analyses. Besides, two different load modes are taken into account herein as: the first case considers only gravity load and the second one is a lumped mass to simulate the moving train, which includes both gravity load and centripetal force. The coordinates along r-axis will be expressed in normalized form as $X = (r - R)/20$, in which r is the distance from the observation point to the original point.

4.1 The effect of curvature on the response

To evaluate the effect of the load's moving curvature on the response, the first case of the load is considered since the amplitude of the load is constant and does not change with the curvature. For the case with frequency f = 30 Hz, f_0 = 20 Hz and c = 70 m/s, the frequency domain vertical displacements along the r-axis on the plane of z = 1 m induced by gravity load along a curve with different radius R = 100 m, 600 m and 10000 m are plotted in Figure 4.

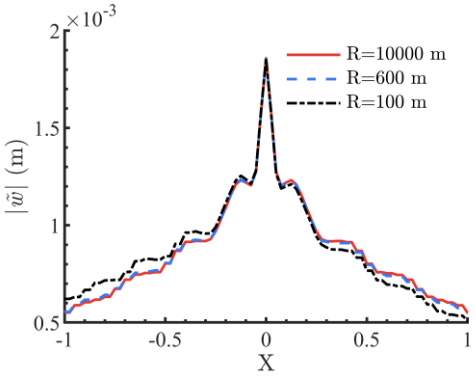

Fig. 4. Response of [R-20, R+20] in frequency domain caused by only gravity load moving along a curve with f = 30 Hz, f_0 = 20 Hz and c = 70 m/s.

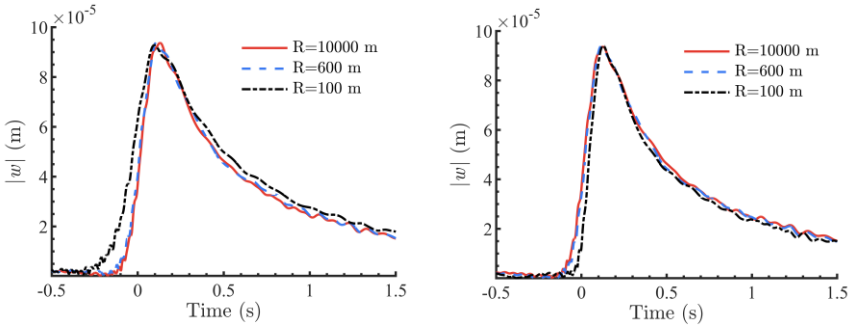

Fig. 5. Response of I-20 and O-20 in time domain caused by the only gravity load moving along a curve with f_0 = 20 Hz and c = 70 m/s:(a) I-20; (b) O-20.

As can be seen, the increment of the curvature increases the response of the inner side of the load movement path and decreases the response of the outer side. The focusing phenomenon caused by curvature can be explained that compared with the case where the load moves in a straight line, the distance between the points on the inner side of the load movement path and the point of load application shortens, resulting in a larger response on the inner side. In addition, the further away from the load point, the more obvious this phenomenon becomes. Another conclusion can be drawn that for the case of the curve radius R = 600 m, the phenomenon mentioned above is not obvious since the curvature for this case is fairly large.

In Figure 5, the vertical responses in time domain at the observation points I-20 and O-20 on the plane of z = 1 m are presented for the case with f_0 = 20 Hz and c = 70 m/s. The influence of curvature can also be observed: As the curvature increases, the response waveform of an inner side point is stretched, while that of an outer side point is compressed. The reason for this phenomenon can be explained in the same way as the frequency-domain response.

4.2 The effect of centrifugal force on the response

In case of a train moving along a curve, gravity load and centripetal force occur simultaneously. To evaluate the effect of centrifugal force on response, the magnitude of frequency-domain displacement components along the r-axis on the plane of z = 1 m caused by a train moving along a curve for the case with different curve radius R and f = 30 Hz, f_0 = 20 Hz and c = 70 m/s are plotted in Figure (6).

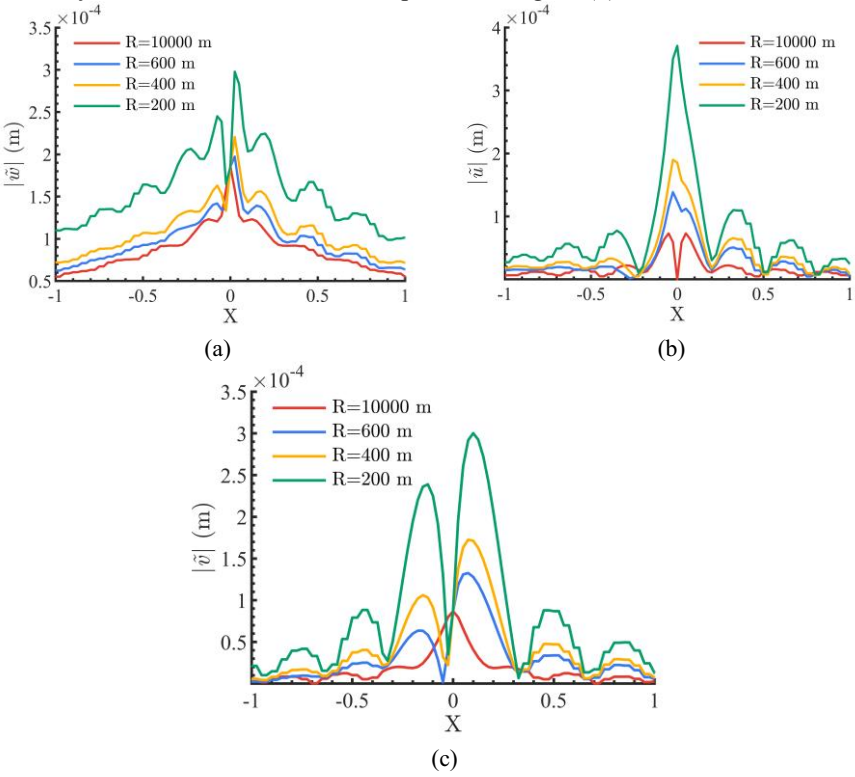

Fig. 6. Response of [R-20, R+20] in frequency domain caused by the train moving along a curve with f = 30 Hz, f_0 = 20 Hz and c = 70 m/s

It can be observed that a larger curvature causes the frequency-domain displacements to increase and the addition of centripetal force amplifies the response on the outer side compared to the inner side. For the responses $|\tilde{w}|$ and $|\tilde{v}|$, those on the outer side is bigger than inner side and the amplitudes of them shift from the center towards the outer side with curvature becoming larger, while their values at X = 0 remain unchanged. For the response $|\tilde{u}|$, the amplitude shifts from both sides to the center, and the responses on the outside of the radius are larger than those on the inside. The aforementioned phenomena can be attributed to centripetal force increasing with the curvature of the moving path. It can be drawn that trains run on paths with a radius exceeding 600 m, variations in $|\tilde{u}|$ and $|\tilde{v}|$ are more pronounced than that in $|\tilde{w}|$.

5 Conclusions

By assuming that the characteristics of a half-space remain invariable in the θ-axis direction, a curved 2.5D model has been proposed to simulate the dynamic response of a half-space caused by a load moving along a curve. In this paper, the 2.5D finite/infinite element method has been incorporated into the cylindrical coordinates, and the derivation for the governing equation of the soil in cylindrical coordinate system has been conducted. Besides, the present method has been proved valid by comparing its results with the analytical ones. Based on the parameter analyses conducted, the main conclusions can be drawn as follows: (1) As for only gravity load moving along a curve, the response exhibits a focusing phenomenon. which becomes more evident as the curvature or distance from the load point increases. (2) The presence of centrifugal force eliminates the focusing phenomenon under load moving along a curve. In the meanwhile, the responses $|\widetilde{w}|$ and $|\tilde{v}|$ on the outer side of the curve exceed those on the inner side. (3) For trains moving along a curve, the centrifugal force should not be disregarded. Moreover, as the curvature increases, the contribution of centrifugal force becomes more remarkable. (4) Compared with trains moving along a straight, the one along a curve have significant changes in responses$|\tilde{u}|$ and $|\tilde{v}|$ due to the centrifugal force, and should be taken seriously. However, the changes in responses $|\widetilde{w}|$ are not significant and can even be ignored.

References

1. Zheng G C and Qi A (2018) State-of-the-art on vibration law and control of buildings adjacent to metro. Earthquake Engineering and Engineering Dynamics., 38:93–102.
2. Ma M and Liu W N (2019) Overview and Key Problem Analysis of the Vibration Influences on Historic Buildings induced by Moving Trains in China. Noise and Vibration Control., 39:1–6.
3. Lamb H (1904) On the propagation of tremors over the surface of an elastic solid. Philosophical Transactions of the Royal Society of London Series A-Containing papers of a mathematical or physical character., 203: 1–42.
4. Eason G (1965) The stresses produced in a semi-infinite solid by a moving surface force. International Journal of Engineering Science., 2:581-609.
5. de Barros F C P and Luco J E (1994) Response of a Layered Viscoelastic Half-space to a Moving Point Load. Wave Motion., 19:189-210.
6. Krylov V V and Ferguson C (1994) Calculation of Low-Frequency Ground Vibrations from Railway Trains. Applied Acoustics., 42:199-213.
7. Taheri M R and Ting E C (1990) Dynamic Response of Plates to Moving Loads: Finite Element Method. Computers & Structures., 34:509–521.
8. He C, Zhou S H, Di H G, Guo P J and Xiao J H (2018) Analytical method for calculation of ground vibration from a tunnel embedded in a multi-layered half-space. Computers and Geotechnics., 99:149–164.
9. Wu Z J, Chen T, Zhao T and Wang L L (2018) Dynamic response analysis of railway embankments under train loads in permafrost regions of the Qinghai-Tibet Plateau. SOIL Dynamics and Earthquake Engineering., 112:1-7.

10. Yang Y B and Hung H H (2001) A 2.5D finite/infinite element approach for modelling visco-elastic bodies subjected to moving loads. International Journal for Numerical Methods in Engineering., 51:1317-1336.
11. Liu W F, Du L L, Liu W N and Thompson D J (2018) Dynamic response of a curved railway track subjected to harmonic loads based on periodic structure theory. Proceedings of the Institution of Mechanical Engineers Part F-Journal of Rail and Rapid Transit., 232:1932–1950.
12. Liu W N, Du L L and Liu W F (2019) Study on Characteristics of Vibration Sources of Metro Trains Running in a Curved Track. Journal of the China Railway Society., 41:26–33.
13. Ma L X, Ouyang H J, Sun C, Zhao R T and Wang L (2019) A curved 2.5D model for simulating dynamic responses of coupled track-tunnel-soil system in curved section due to moving loads. Journal of Sound and Vibration., 451:1–31.
14. Yang Y B, Liu S J, Chen W, Tan Q and Wu Y T (2021) Half-space response to trains moving along curved paths by 2.5D finite/infinite element approach. Soil Dynamics and Earthquake Engineering., 145.